CONF-901025--19

INTERNATIONAL ATOMIC ENERGY AGENCY

THIRTEENTH INTERNATIONAL CONFERENCE ON
PLASMA PHYSICS AND CONTROLLED NUCLEAR FUSION RESEARCH

Washington, DC, United States of America, 1-6 October 1990

IAEA-CN--53/C-3-2

DE91 002328

STABILIZATION OF THE INTERCHANGE MODES BY A MAGNETIC AXIS SHIFT AND A TOROIDAL FIELD IN HELIOTRON E, AND A NEW LOW-N MODE STABILITY ANALYSIS

M.WAKATANI, H.ZUSHI, F.SANO, S.SUDO, M.HARADA, T.MIZUUCHI, K.KONDO, M.SATO, S.BESSHOU, H.OKADA, Y.NAKAMURA, K.ICHIGUCHI, H.SUGAMA*, T.OBIKI*
Plasma Physics Laboratory, Kyoto University, Gokasho, Uji, Japan

B.A.CARRERAS, N.DOMINGUEZ, J.N.LEBOEUF, V.E.LYNCH
Oak Ridge National Laboratory, Oak Ridge, Tennessee, USA

J.L.JOHNSON, G.REWOLDT
Plasma Physics Laboratory, Princeton University, Princeton, New Jersey, USA

* *Present address : National Institute of Fusion Science, Nagoya, Japan.*

DISCLAIMER

ABSTRACT

STABILIZATION OF THE INTERCHANGE MODES BY A MAGNETIC AXIS SHIFT AND A TOROIDAL FIELD IN HELIOTRON E, AND A NEW LOW-N MODE STABILITY ANALYSIS.

Pressure-driven MHD instabilities in Heliotron E were studied by shifting the vacuum magnetic axis position outward ($\Delta_v > 0$) or inward ($\Delta_v < 0$), and/or applying an additional toroidal field additively or subtractively. The global behaviors of experimental results are consistent with theoretical studies using the ideal and the resistive MHD model based on the stellarator expansion approximation. The pressure profile was also changed systematically by the above control of the vertical magnetic field and/or the toroidal field. Stability improvement was obtained for the $\beta(0) \lesssim 1\%$ regime in the case where the additive toroidal field was (3-8)% of the toroidal component from the helical coils for -2cm $\leq \Delta_v \leq$ 0cm. It is believed that the pressure profile was unintentionally adjusted to improve stability; however this improvement was not clear for $\beta(0) \gtrsim (2-3)\%$.

A new type of ideal low-n stability code was developed which relies on an averaging procedure in the toroidal direction of a three dimensional finite beta MHD equilibrium. This approach seems to include realistic finite beta configuration in the stability calculation better than the usual stellarator expansion method. For the Heliotron E the difference between both results is fairly small.

1. INTRODUCTION

Previous confinement studies on Heliotron E have been extended by changing the vacuum magnetic configuration to stabilize the ideal and resistive interchange modes. Two method have been proposed to improve the beta limit of Heliotron E. One is to produce a sufficiently deep magnetic well by shifting the magnetic axis outward[1]. The other is to apply an additional toroidal magnetic field for shifting the $\iota = 1$ surface resonant with the (m,n)= (1,1) mode into an outside region where shear stabilization is expected[2]. High beta experiments were tried again to study these theoretical predictions and to improve the beta limit considerably by using both additional vertical field coils and nineteen toroidal field coils. Finite beta plasmas were produced by injecting NBI (maximum power is 2.5 MW) into the target ECRH plasmas at $B_{tot} = B_{ho} + B_{to} = 1.9\ T$ or $B_{tot} = 0.94\ T$, where B_{ho} and B_{to} are toroidal fields at the center of the vacuum chamber produced by the helical coils and the toroidal coils, respectively.

The main purpose of this paper is to compare the results of the new high beta experiment with the recent theoretical stability analyses including the realistic vacuum magnetic configuration of Heliotron E. For the ideal MHD stability mainly we use the STEP code modified to include the toroidal corrections correctly[3,4]. We have already compared the STEP code results for low-n mode stability with the FAR code[5] and for the Mercier criterion with the VMEC code[6]. For the resistive modes an initial value solver (RESORM code) was developed for the equilibrium given by the STEP code[7]. It is known that the beta limit determined by the low-n ideal interchange mode is somewhat higher than that given by the Mercier cri-

terion[8,9]. Also the resistive interchange mode is always unstable in the magnetic hill region that is inevitable in the heliotron/torsatron configuration. Based on the comparison between the data and the theoretical studies, the experimental beta value exceeds the Mercier criterion and is close to the low-n ideal interchange limit when the Mercier limit is low or $\beta_c(0) \lesssim 1\%$. However, when $\beta_c(0) > 1\%$, the sawtooth oscillations correlate well with the low-n resistive interchange mode growth rate, γ_g. Roughly $\gamma_g \simeq 0.01$ at $S = 10^6$ normalized with respect to the poloidal Alfven transit time gives a good measure for the appearance of the sawtooth oscillations. Here S is a magnetic Reynolds number. It is noted that $\gamma_g \simeq 0.01$ is obtained always above the Mercier limit in Heliotron E. This conjecture is also consistent with the Heliotron DR data[7].

In §2 we discuss results of the magnetic axis control experiment and compare them with the theoretical stability analysis. In §3 results of the additional toroidal field experiment are shown and compared with the theoretical predictions based on ideal and resistive MHD. Here a parameter $\alpha^* \equiv B_{to}/B_{ho}$ is changed from $\alpha^* = 0.1$ to $\alpha^* = -0.1$.

Recent development of three-dimensional MHD codes has made MHD equilibrium calculations of heliotron/torsatron efficient. Two-dimensional numerical codes, such as the STEP and FAR codes, are efficient for study of the linear MHD stability properties of heliotron/torsatron. It is natural to combine both types of codes to study global stability in three-dimensional configurations[4]. We have coupled the VMEC code for MHD equilibrium with the STEP code for low-n ideal mode stability, introducing numerical averaging procedures to transfer the equilibrium data to the stability code. In §4 results from this new VMEC-STEP code are shown and compared with the STEP code for Heliotron E.

2. MAGNETIC AXIS CONTROL EXPERIMENT

In Heliotron E the magnetic axis position can be controlled by changing the vertical field. MHD stability theory predicts that the magnetic well is deepened by outward shift, which improves the stability beta limit. On the contrary an inward shift of the magnetic axis degrade the stability. Figure 1 shows the MHD stability diagram in the $\beta(0) - \alpha^*$ plane for n = 1 and n = 3 global modes and the Mercier mode at the flux surfaces resonant with these modes for $\Delta_v = -2cm, \Delta_v = 0cm$ and $\Delta_v = 2cm$. The pressure profile $P \propto (1 - \psi)^2$ is assumed, where ψ is a poloidal flux function. The points for the low-n mode stability show $\gamma_I = 0.01$ and $\gamma_g = 0.01$ at $S = 10^6$, where γ_I and γ_g are growth rates of the ideal and resistive modes normalized by the poloidal Alfven time, respectively. If we consider $\gamma_I = 0$ for the low-n ideal mode, it should coincide with the Mercier limit.

Figure 2 (a) shows the oscillations on the soft X-ray signal, I_{sx}, for several cases with an inward magnetic axis shift. Here discharges with $\beta(0) < 1\%$ or $B_{tot} = 1.9\ T$ were selected. For the standard case with $\Delta_v = 0$, the sawtooth like oscillations were never observed for $\beta(0) < 1\%$. At $\Delta_v = -2cm$ the sawtooth amplitude is $\Delta I_{sx}/I_{sx} \sim 60\%$, and at $\Delta_v = -4cm$ $\Delta I_{sx}/I_{sx} \lesssim 10\%$; however, the sawtooth repetition time reduces to $(2 \sim 3)msec$ compared to $\sim 10msec$ at $\Delta_v = -2cm$. For the outward shift case of $0 < \Delta_v \lesssim 4cm$, there were no detectable oscillations on the soft X-ray for $\beta(0) < 1\%$. These results are consistent with the stability diagram in Fig.1. The large sawtooth at $\Delta_v = -2cm$ occurred near the $\iota = 1/2$ surface (see Fig.2(b)). This is a new phenomenon observed with an inward axis shift,

and is expected from Fig.1. Also post-cursor oscillations with (m,n) =(2,1) were observed on the soft X-ray signal, which means that the m = 2 magnetic islands survive after the crash of the sawtooth. This shows a role of the resistive interchange mode, since resistive reconnection is required to produce the magnetic islands. Figure 2(b) shows the phase inversion radius of the sawtooth as a function of Δ_v. Circles correspond to gas puffed discharges with $\beta(0) < 1\%$ and triangles belong to $1\% < \beta(0) < 3\%$ obtained by pellet injection. Resonant surfaces with $\iota = 1/2$, 2/3 and 1(or q=2, 3/2 and 1) at $\beta(0) = 0\%$ and separation lines between the magnetic well and the magnetic hill at$\beta(0) = 0\%$, 2% and 3% are shown . Figure 2(b) clearly shows that the phase inversion radius of the sawtooth for the higher beta plasmas appears in the outer region where the $\iota = 2/3$ and $\iota = 1$ surfaces exist. One explanation is that the resistive interchange modes at the $\iota = 1/2$ surface which trigger the sawtooth for $\beta(0) < 1\%$ and $\Delta_v \simeq -2cm$ are stabilized by the expansion of magnetic well region and the pressure profile broadening associated with the increase of $\beta(0)$.

3. STABILITY PROPERTIES WITH ADDITIONAL TOROIDAL FIELD

When a toroidal field is added to decrease the rotational transform or $\alpha^* > 0$, the outermost flux surface expands to increase the average plasma radius, $\bar{a}$. For $\alpha^* > 0$, if $\bar{a}$ is held fixed for a given peaked pressure profile, the dangerous resonant surface with $\iota = 1$ moves outwards or the pressure gradient at the $\iota = 1$ surface decreases. Under this situation the ideal MHD stability for the $n = 1$ mode improves significantly[2]. In the Heliotron E experiment a material limiter was not used to fix $\bar{a}$. The $\gamma_I = 0.01$ and $\gamma_g = 0.01$ points shown in the $\beta(0) - \alpha^*$ plane in Fig.1 are with the variation of $\bar{a}$. It is noted that the toroidal field with $\alpha^* < 0$ increases the rotational transform and decreases $\bar{a}$. For $\alpha^* < 0$ the stability degrades compared to $\alpha^* = 0$ (standard case) and for $\alpha^* > 0$ the stabilizing effect is milder than the results in ref.[2]. Figure 3 shows experimental results for various α^* under the condition of $\Delta_v = -2cm$ and $\beta(0) < 1\%$. As discussed in Section 2 the sawtooth oscillations appear ever for $\beta(0) < 1\%$ under $\alpha^* = 0$ and $\Delta_v < 0$. The sawtooth amplitude is enhanced by $\alpha^* < 0$. We note that, when $0.03 \leq \alpha^* \leq 0.08$, the sawtooth oscillations were suppressed. For $\alpha^* > 0.1$, however, they appeared again. Other important characteristic of the α^* effect is that the peaking factor of the density profile is changed as shown in Fig.4(a). This factor $n_e(0)/ < n_e >$ can be controlled about a factor of two in the range of $0 \leq \alpha^* \leq 0.1$. However, the electron temperature profile was almost same for $-0.1 < \alpha^* < 0.1$. From the STEP and RESORM code results, when the pressure profile becomes broad, the stability beta limit increases. For $\alpha^* \gtrsim 0.1$, the plasma radius expands excessively and the plasma-wall interaction becomes strong, which was shown by the spectroscopic measurements of impurity lines. This may suggest that the temperature profile at $\alpha^* = 0.1$ becomes relatively sharp compared to that in $0.03 \leq \alpha^* \leq 0.08$. This means that the pressure profile becomes peaked again, since $n_e(0)/ < n_e >$ is almost constant for $\alpha^* \gtrsim 0.08$. From the stability diagrams shown in Fig.1, $\alpha^* > 0$ and $\Delta_v > 0$ is sufficient to obtain $\beta(0) \gtrsim 3\%$ by the condition of $\gamma_I = 0.01$. However, for Δ_v = -2cm, $\beta(0) \sim 3\%$ may not be expected. The experiment to improve the beta limit at $\Delta_v = 2cm$ was tried but degradation of confinement limited the beta value to $\beta(0) \lesssim (1 \sim 2)\%$.

Magnetic fluctuations were measured by using magnetic probes inside the vacuum chamber.

Usually $\tilde{B}_\theta$ with (m,n) = (1,1) was observed at $f \simeq 11kHz$ for almost all high beta discharges. This coherent magnetic fluctuation was usually dominant even though the (m,n)=(2,1) or (m,n)=(3,2) mode was observed clearly on the soft X-ray fluctuation and the line density fluctuations (see Fig.3). Figure 4(b) shows $\tilde{B}_\theta$ as a function of α^* at $\Delta_v = -2cm$ for $1\% \leq \beta(0) \leq 3\%$. In this case the (m,n)=(2,3) mode is dominant and stronger than the (m,n)=(1,1) mode. Since the pressure profile becomes broad because of the carbonization of the wall for $0.03 \leq \alpha^* \leq 0.08$, the pressure gradient becomes large at the $\iota = 3/2$ resonant surface which excites the (m,n)=(2,3) resistive interchange mode. We note that this magnetic fluctuation is large where the stability improvement is observed for $\beta(0) < 1\%$ plasmas (see Fig.3).

4. A NEW LOW-N MODE STABILITY ANALYSIS

We have developed a new code to study low-n ideal mode stability by coupling the VMEC code to the STEP code. In the VMEC code, the magnetic field is described by $\mathbf{B} = \nabla s \times \nabla(\psi'\vartheta - \chi'\zeta - \lambda)$, where ζ means the angle in the toroidal direction, ψ and χ are a toroidal and a poloidal flux, respectively. The prime denotes the derivative with respect to s. Since space coordinates (R,Z) and λ are related to (s,θ,ζ), the magnetic field components are given by $B_R = B^\theta \frac{\partial R}{\partial \theta} + B^\zeta \frac{\partial R}{\partial \zeta}$, $B_Z = B^\theta \frac{\partial Z}{\partial \theta} + B^\zeta \frac{\partial Z}{\partial \zeta}$, and $B_\phi = B^\zeta R$, where $B^\theta = (\chi' - \frac{\partial \lambda}{\partial \zeta})/\sqrt{g}$ and $B^\zeta = (\psi' - \frac{\partial \lambda}{\partial \theta})/\sqrt{g}$. On the other hand the magnetic field in the STEP code is given by $\mathbf{B} = \nabla s \times \nabla(\psi'\hat{\theta} - \chi'\phi)$, where $\hat{\theta} = \theta - \lambda(s,\theta,\zeta)/\psi'$ which gives straight magnetic field lines on the $(\hat{\theta},\phi)$ plane. By numerical calculations we find the correspondence between θ and $\hat{\theta}$. Using $\hat{\theta}$, we obtain $\{R(s,\hat{\theta},\phi), Z(s,\hat{\theta},\phi)\}$ and $\mathbf{B} = \{B_R(s,\hat{\theta},\phi), B_Z(s,\hat{\theta},\phi), B_\phi(s,\hat{\theta},\phi)\}$. We apply the averaging procedure over the ϕ coordinate, and obtain $\{\bar{R}(s,\hat{\theta}), \bar{Z}(s,\hat{\theta})\}$ and the magnetic curvature term

$$\Omega(s,\hat{\theta}) \equiv \frac{\overline{R^2}}{R_o^2} - \frac{\overline{B_\delta^2}}{B_o^2} - 1,$$

where the bar means the averaged quantity. Here B_δ is the nonaxisymmetric stellarator magnetic field, and R_o and B_o are taken at the center between the two helical coils of Heliotron E. By constructing a $\{\psi,\theta\}$ coordinate system from $\{\bar{R},\bar{Z}\}$ for the STEP code, we have combined the VMEC equilibrium code with the STEP low-n stability analysis. Figure 5 shows the comparison between the STEP code and the new VMEC-STEP code for the ideal n=1 mode in Heliotron E. Both the growth rates and the threshold beta value show good agreement. We think that the VMEC-STEP code is useful for study of the stability of torsatrons with a low aspect ratio or helical pitch number, since the VMEC code gives realistic three-dimensional finite beta equilibrium data such as the position of resonant surface, magnetic shear and local average curvature to the STEP stability solver.

Acknowledgement

Theoretical works were supported by US-Japan Cooperative Stellarator/Heliotron Program and JIFT Program.

References

[1] WAKATANI,M., et al., in Plasma Physics and Controlled Nuclear Fusion Research 1986(Proc. 11th Int. Conf. Kyoto, 1986)vol.2, IAEA, Vienna(1987)625.

[2] CARRERAS, B.A., et al., ibid, p.615.

[3] ANANIA,G., JOHNSON,J.L., WEIMER,K.E., Phys.Fluids 26(1983)2210.

[4] NAKAMURA,Y., et al., J.Phys. Soc. Jpn 58(1989)3157.

[5] LYNCH,V.E., et al., J.Comp. Phys. 66(1986)411.

[6] HIRSHMAN, S.P., van Rij, W.I., MERKEL,P., Comput. Phys. Commun 43(1986)143.

[7] ICHIGUCHI,K., et al., Nucl.Fusion 29(1989)2093.

[8] DOMINGUEZ,N., et al., Nucl.Fusion 29(1989)2073.

[9] SUGAMA,H., WAKATANI,M., J.Phys.Soc.Jpn 58(1989)1128.

Figure Captions

Fig.1 Mercier limit (continuous line) for the resonant surfaces with $\iota = 0.5, 0.6, 0.75$, or 1.0 is shown in $\beta(0) - \alpha^*$ plane for $\Delta_v = -2cm, \Delta_v = 0cm$ and $\Delta_v = 2cm$. $\gamma_I = 0.01$ (circles) and $\gamma_g = 0.01$ at $S = 10^6$ (squares) for the assigned dominant mode are plotted, where γ_I and γ_g are growth rates of the ideal and resistive modes normalized by the poloidal Alfven transit time, respectively, and S is a magnetic Reynolds number. Pressure profile is fixed at $P \propto (1 - \psi)^2$, where ψ is a poloidal flux function.

Fig.2(a) Soft X-ray traces for various Δ_v cases at $\alpha^* \equiv B_{to}/B_{ho} = 0$. Both central and edge chords are shown. (b)Phase inversion radius of soft X-ray signal at the sawtooth crash as a function of Δ_v at $\alpha^* = 0$. Circles and triangles show low beta case ($\beta(0) < 1\%$) and high beta case ($1\% < \beta(0) \lesssim 3\%$), respectively. Resonant surfaces and separation lines between magnetic well and magnetic hill are shown.

Fig.3 Time evolution of line averaged density(left) and soft X-ray(right) along the central chord for various $\alpha^* \equiv B_{to}/B_{ho}$ at $\Delta_v = -2cm$. One division corresponds to 15 msec. Here all cases belong to $\beta(0) < 1\%$.

Fig.4(a) Peaking factors given by $n_e(0)/ < n_e >$ are shown as a function of α^* for $\beta(0) < 1\%$ plasmas. In the dotted regions sawtooth type oscillations were observed. (b)Magnetic fluctuations showing the coherent $(m, n) = (3, 2)$ mode are shown as a function of α^* for plasmas with $1\% < \beta(0) < 3\%$.

Fig.5 Growth rates of the n = 1 mode versus $\beta(0)$ by VMEC-STEP code ($S = \infty$), STEP code ($S = \infty$) and RESORM code($S = 10^6$) for Heliotron E standard configuration ($\alpha^* = 0$ and $\Delta_v = 0$).

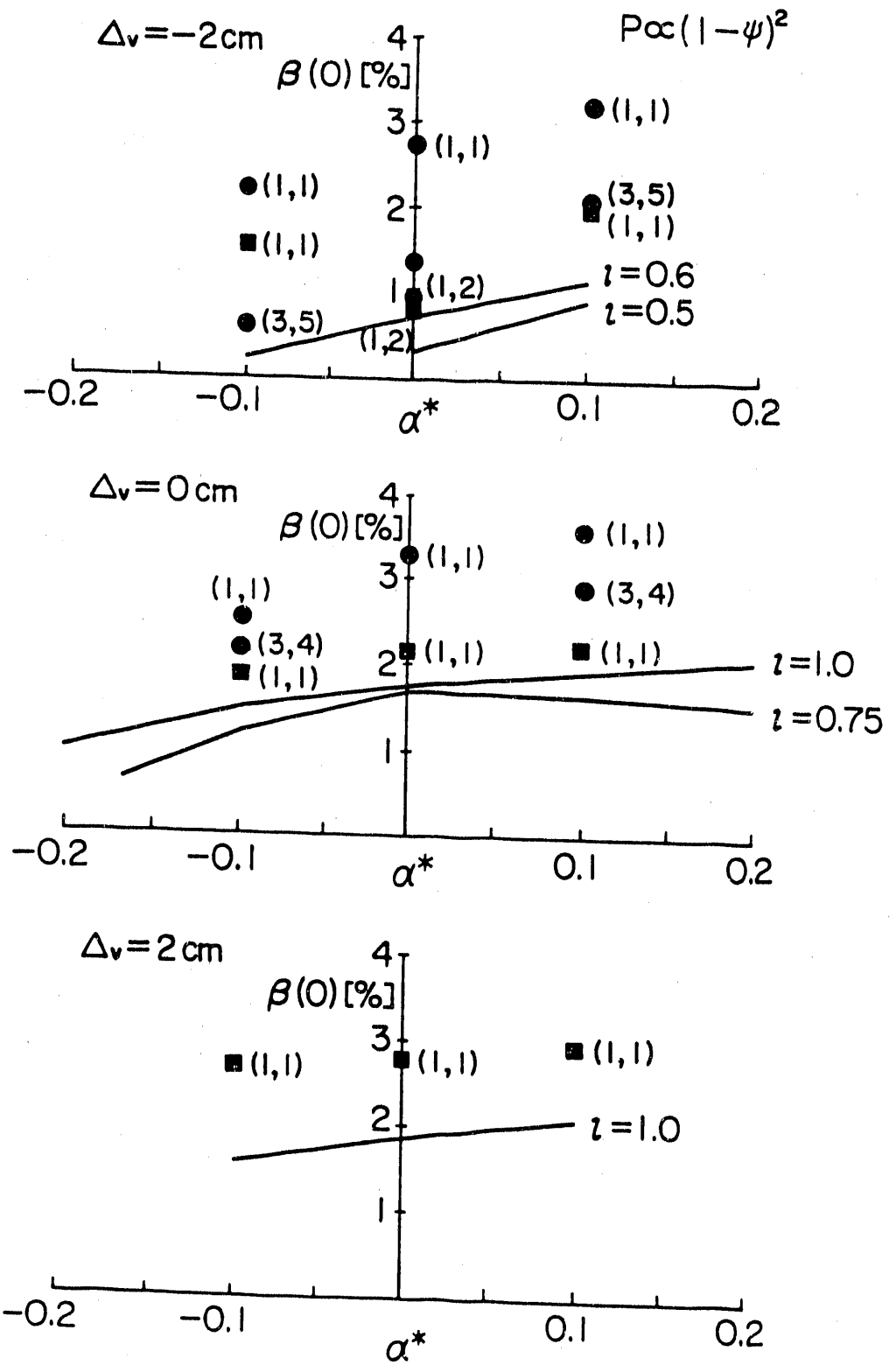
Δv=−2cm
Pαc(1−ψ)²
β(0)[%]
4
3
2
1
(1,1)
(1,1)
(1,1)
(1,1)
(3,5)
(1,1)
(1,2)
(3,5)
(1,2)
l=0.6
l=0.5
−0.2
−0.1
α*
0.1
0.2
Δv=0cm
β(0)[%]
(1,1)
(1,1)
(3,4)
(3,4)
(1,1)
(1,1)
(1,1)
l=1.0
l=0.75
Δv=2cm
β(0)[%]
(1,1)
(1,1)
(1,1)
l=1.0

Fig. 1

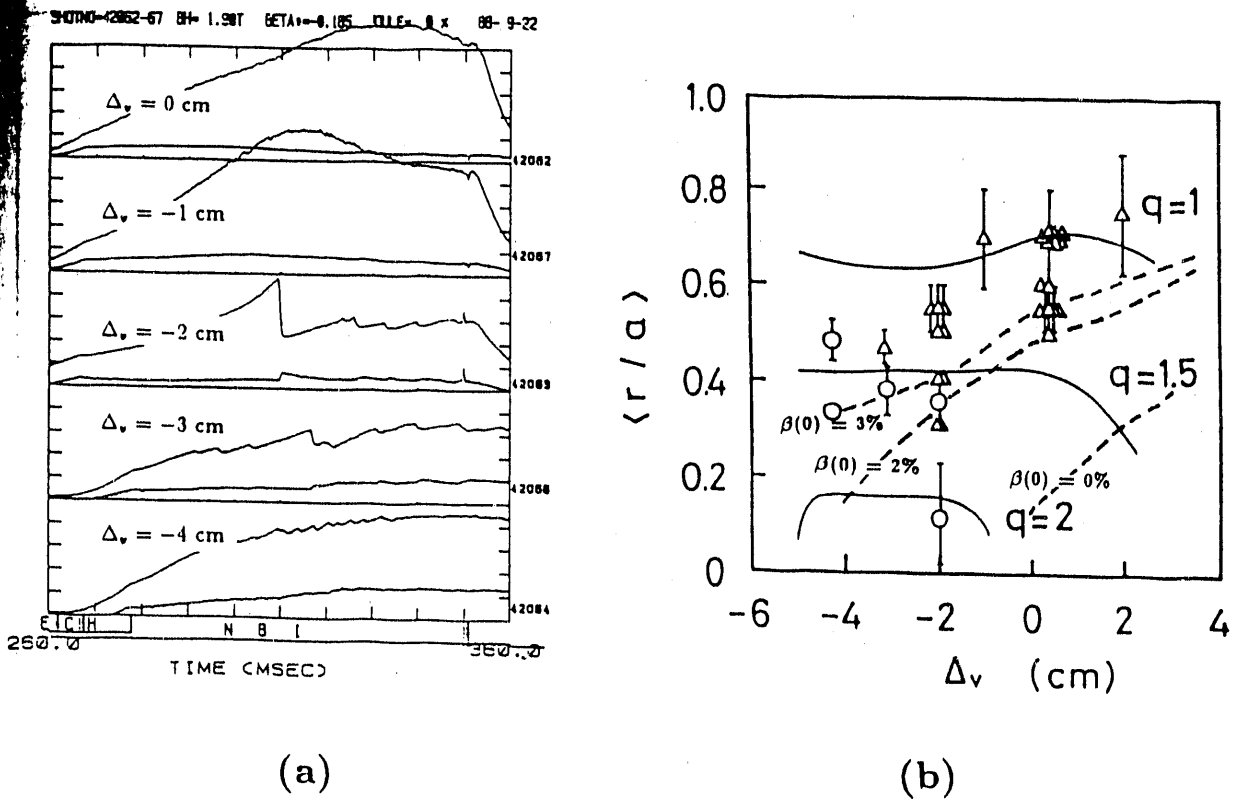
Δv = 0 cm
Δv = −1 cm
Δv = −2 cm
Δv = −3 cm
Δv = −4 cm
42062
42067
42069
42068
42064
E C H
N B I
260.0
360.0
TIME (MSEC)
1.0
0.8
0.6
0.4
0.2
0
⟨r / a⟩
q=1
q=1.5
q=2
β(0) = 3%
β(0) = 2%
β(0) = 0%
-6
-4
-2
0
2
4
Δv (cm)

(a) (b)

Fig. 2

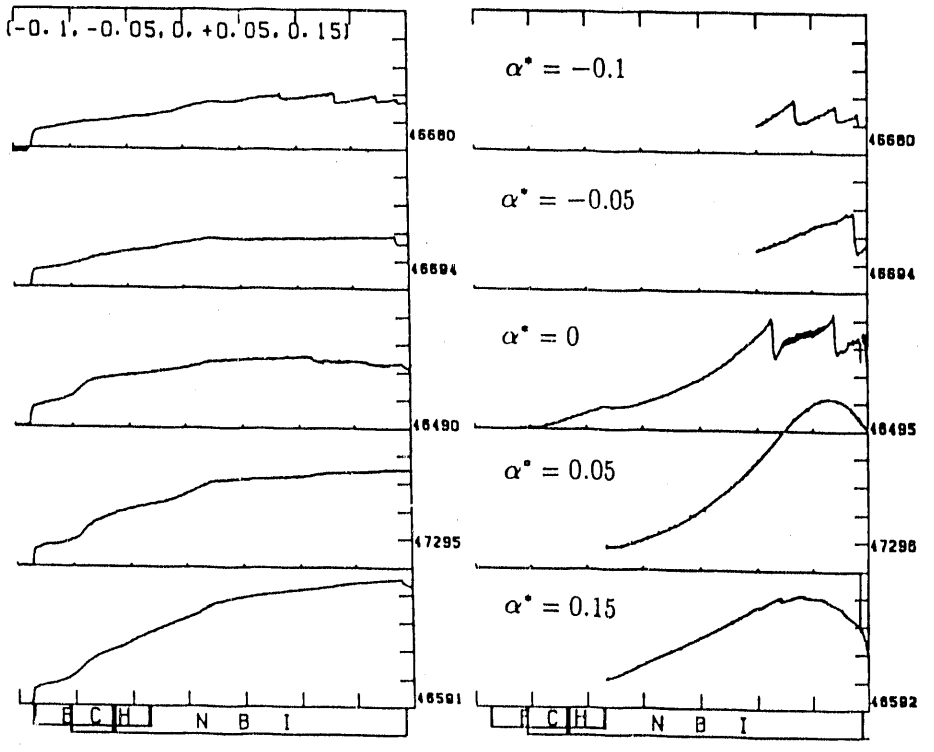
(-0.1, -0.05, 0, +0.05, 0.15)
α* = −0.1
α* = −0.05
α* = 0
α* = 0.05
α* = 0.15
46680
46694
46490
47295
46591
46680
46694
46495
47298
46592
E C H
N B I
E C H
N B I

Fig. 3

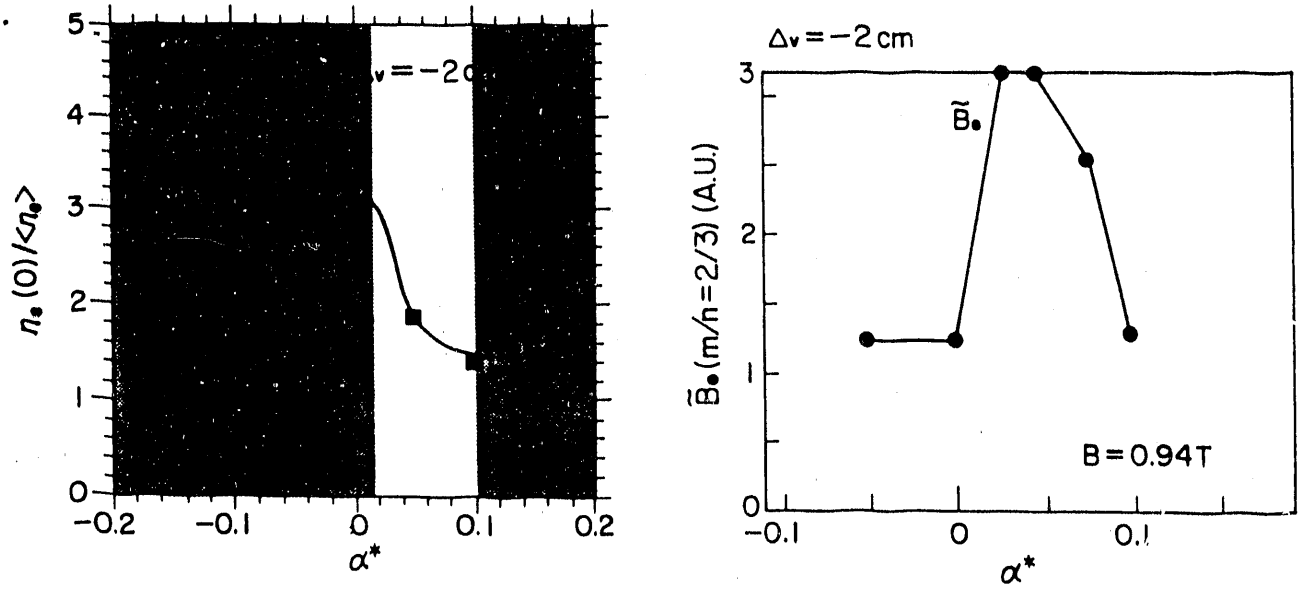
$n_e(0)/\langle n_e \rangle$
α^*
$\Delta v = -2$ cm
$\tilde{B}_\theta$
$\tilde{B}_\theta$ (m/n=2/3) (A.U.)
B=0.94T
α^*

(a) (b)

Fig. 4

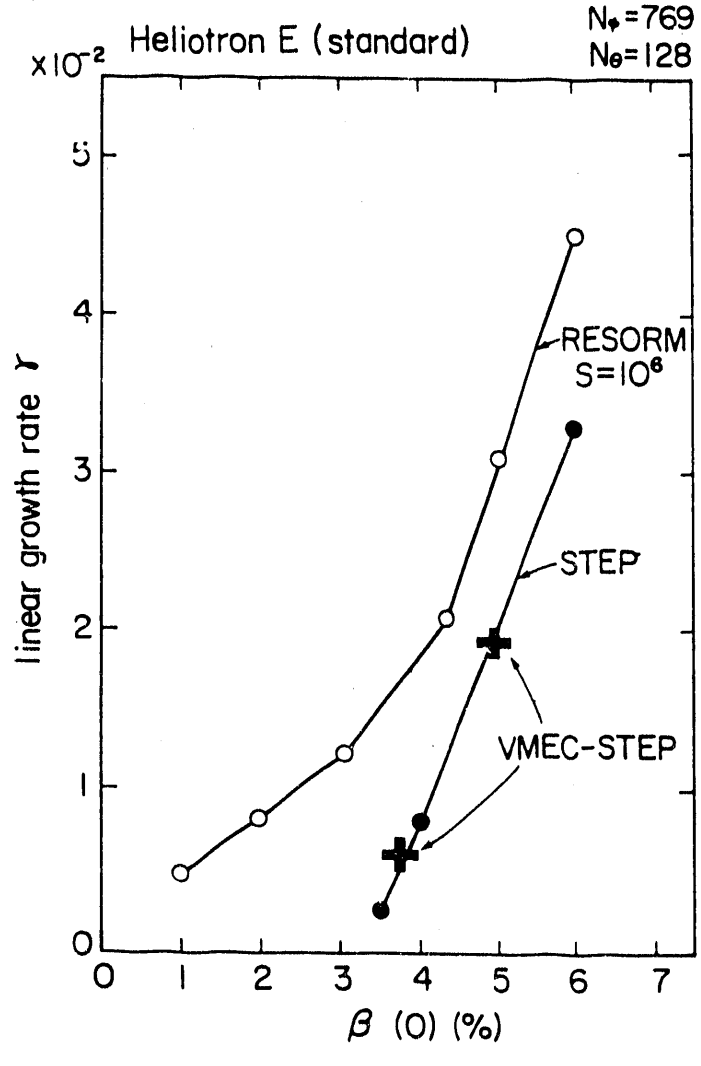
Heliotron E (standard)
N_ϕ=769
N_θ=128
$\times 10^{-2}$
linear growth rate γ
RESORM
S=10^6
STEP
VMEC-STEP
β (0) (%)

Fig. 5

- END -

DATE FILMED

11 / 28 / 90